10.1109/LAWP.2017.2783943

Fractal-Shaped Metamaterial Absorbers for Multi-Reflections Mitigation in the UHF-Band

F. Venneri, *Member, IEEE*, S. Costanzo, *Senior Member, IEEE*, G. Di Massa, *Life Member, IEEE*

***Abstract*— A Minkowski fractal geometry is proposed in this work as miniaturized absorber cell suitable for multipath phenomena mitigation within the European RFID UHF-band. The proposed structure is analyzed through the combined use of an equivalent transmission line model and MoM-based full-wave simulations. Very high miniaturization capabilities (about 50% with respect to standard configurations) are demonstrated for a 868MHz absorber unit cell, characterized by an absorptivity more than 99%, a good angular stability and a very thin substrate ($\leq\lambda_0/100$). The proposed configuration is appealing for designing compact absorbers useful for multipath reduction in wireless systems operating on restricted indoor environments.**

***Index Terms* - Fractals, microwave absorbers, UHF-RFID.**

I. Introduction

Wireless technologies are integral part of daily life, and they are continuously evolving towards better quality services. Actually, they appear in different contexts, such as in medicine, public safety, and logistics applications. Furthermore, wireless systems are gaining growing interest in various commercial/manufacturing applications involving indoor areas, such as stores and warehouses. However, indoor locations represent a hostile environment for radio communications, which are typically affected by multiple reflection interferences. Various multipath propagation models have been developed for mobile communications and for some indoor wireless systems, such as WLAN [1]. However, only a few early studies have been devoted to multipath propagation in RFID systems [2]. Practical techniques are needful to prevent incorrect readings of RFID tags within indoor areas [3]. To this end, microwave absorbers can provide an effective hardware solution to reduce multipath interferences. However, the size of traditional microwave absorbing materials is too large. Furthermore, in the UHF band, conventional $\lambda/4$-thick Salisbury screens are very bulky, whereas ferrite-based absorbers are heavy and expensive [4]. Recently, metamaterial absorbers (MAs) have been proposed as lightweight and space-saving solution to improve the reliability of UHF-RFID systems: a 920 MHz optically transparent MA is proposed in [4]; a low-cost MA is designed in [5, 6] for European RFID bands, and a miniaturized MA cell with four lumped resistors is shown in [7]. MAs were introduced for the first time by Landy et al.in [8]. They consist of a periodic metallic pattern printed on a low-loss and thin grounded substrate, synthesized to perform perfect absorption around a given frequency. Since its first demonstration, MAs have been adopted in several applications throughout electromagnetic spectrum [9].

In this Letter, the fractal based MA configuration preliminarily introduced by the authors in [10] is adopted as a valid solution for multipath reduction in UHF-RFID systems. The Minkowski geometry, yet adopted by the authors in reflectarrays [11, 12], is investigated to obtain a thin and miniaturized MA unit cell, to be fruitfully exploited for multi-reflections mitigation in confined indoor areas. Actually, the intrinsic miniaturization capabilities of fractals allow to obtain UHF-absorbing panels having denser lattices and smaller sizes when compared to both traditional microwave absorbers as well as to the existing MA configurations specifically designed for UHF-band [4-6]. The structure presented in this Letter allows to obtain very small unit cells (about 40-65% smaller than those designed in [4-6]). Furthermore, it offers quite good miniaturization levels without using any lumped resistors and adopting a thinner substrate, that is $\lambda_0/100$ at the operating frequency, against the $\lambda_0/15$ thickness used in [7]. Useful design rules are retrieved from the analysis stage through the combined use of an equivalent transmission line model [13] and full-wave simulations. Good miniaturization capabilities, very high absorptivity and good angular stability are demonstrated. Furthermore, future multiband developments of proposed MA configuration are outlined in the conclusions.

II. Fractal MA Cell and Equivalent Circuit Model

The proposed MA configuration is depicted in Fig. 1. It consists of a periodic array of fractal patches printed on a thin grounded dielectric slab (Fig. 1(a)). The unit cell is based on the use of a 1st order Minkowski patch (Fig. 1(b)). It is characterized by a beginning square element of sizes L×L, which is modified by removing a smaller SL×SL square from the centre of its sides. S is the scaling factor, variable in the range from 0 up to 1/3 [11]. The main benefit related to the adoption of fractal geometries in the design of microstrip patches is due to the fact that a greater electrical length can be fitted into a smaller physical area. In the case of the adopted Minkowski patch, for example, the resonant length, nearly equal to (1+2S)L [12], is longer as compared to that given by the beginning square patch. Of course, the increased electrical length of fractal resonators leads to a lower resonant frequency, so that the patch must be miniaturized in order to move the resonance up to the desired working frequency.

Manuscript received November 13, 2017.

The authors are with the Università della Calabria, 87036 Rende, Italy (e-mail: costanzo@dimes.unical.it)

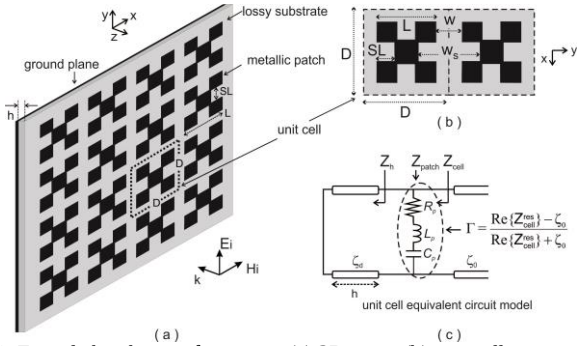

Fig. 1. Fractal absorber configuration: (a) 3D view; (b) unit cell geometry; (c) equivalent circuit model of the unit-cell [10, 13].

In this work, the proposed 1st order fractal shape is synthesized for perfect absorption, namely to realize the matching between MA unit cell and free space impedances at a given resonant frequency f_0. Both degrees of freedom inherent to the adopted Minkowski shape, i.e. the length L and the inset size SL (Fig. 1(b)), are properly exploited to satisfy the above conditions, achieving good miniaturization features.

In order to give a physical explanation of the mechanism assuring the matching between the fractal unit cell and free space impedances, an equivalent transmission line (TL) model is adopted (Fig. 1(c)) as a simple analysis tool [13]. The model is adopted to evaluate the unit cell input impedance behavior against fractal shape variations, so disclosing how fractal geometric/electrical parameters can accomplish perfect absorption condition at a given resonant frequency. To this end, the unit cell is modeled through an impedance Z_{cell} (Fig. 1(c)) given by the parallel combination of the grounded substrate impedance Z_h [13] and a series RLC-circuit, which represents the patch impedance, given as:

$$Z_{patch} = R_p + \frac{\left(1-\omega^2 L_p C_p\right)}{j\omega C_p} \qquad (1)$$

In the above formula, R_p takes into account for ohmic/dielectric losses; L_p and C_p represent the inductance and the capacitance of the cell, respectively due to: the magnetic flux between the patch and the ground plane; the parasitic capacitance between the edges of adjacent patches and the capacitance between the patch and the ground plane due to the evanescent Floquet modes, in the case of thin substrates (h<0.3D) [13]. The above lumped parameters are numerically retrieved through a full-wave simulation of the unit cell reflection coefficient [13]. Closed-form expression are also available in [14] for square patches. As demonstrated in [13], the TL-model reveals that, for a fixed substrate, the real part of the input impedance at the resonance is essentially an increasing function of the unit cell capacitance C_p. So, as discussed in the following section, a proper tuning of C_p allows to achieve perfect absorption condition (i.e. $\mathrm{Re}\{Z_{cell}^{res}\} = 377\Omega$). To better understand the physical meaning of numerically computed C_p-values, the electrostatic principles are considered. In fact, by observing the expression of the static capacitance of an ideal parallel plate capacitor with a plate area A and a plate separation d (i.e. $C=\varepsilon_0\varepsilon_r A/d$) [13], the effect of the fractal dimensions variations on the unit cell capacitance C_p and impedance can be easily retrieved.

III. Design of Fractal MAs for UHF-RFID Band

Fractal MAs based on the use of a common FR4 substrate (ε_r=4.4, tanδ=0.02, h=3.2mm≅λ_0/100) are designed to operate in the UHF-RFID band around the frequency f_0=868 MHz. A commercial full-wave code, based on the infinite array approach, is adopted as design tool assuming a normally impinging plane-wave. Furthermore, an equivalent TL-model is implemented for unit cells analysis (Fig. 1(c)). In order to derive some useful design rules for the proposed MA configuration, the input impedance Z_{cell} and the absorptivity, $A(\omega)=1-|\Gamma|^2$, of some unit cell samples are reported in Fig. 2. The above input parameters are computed versus frequency, for a fixed unit cell size D equal to $\lambda_0/4$, by varying the patch length L from 62mm up to 79mm. A variation of the scaling factor S is imposed from 0 up to 0.3. Fig. 2 also illustrates the unit cells input impedance and absorptivity, computed through the TL-model, considering the capacitances/inductances values reported in Table I; these are retrieved from a full-wave simulation of each cell [13]. A good agreement can be observed between MoM and TL-model results, confirming the correctness of the computed lumped parameters R_p, L_p and C_p. Data reported in Fig. 2 provide an exhaustive description of the absorption mechanism on the basis of the proposed MA, by also highlighting the intrinsic miniaturization capabilities of fractal with respect to the beginning square shape (i.e. S=0). As a matter of fact, Fig. 2 shows that by increasing the scaling factor S from 0 up to 0.3, for a fixed patch size L, the cell resonant frequency is shifted down, because the effective fractal length increases [11]. Accordingly, the same resonance frequency, for example f_0=868MHz, can be achieved by adopting a square patch (i.e. L=79mm-S=0), or alternatively, by using a fractal patch with reduced sizes (e.g. L=67mm-S=0.21 or L=62-S=0.25). Furthermore, Fig. 2(a) demonstrates how the use of greater S-values reduces the cell impedance, namely the cell capacitance C_p (Table I), so allowing the free-space matching. This happens because the parallel plate capacitor formed by two adjacent patches has an increasing distance in correspondence of the inset SL (i.e. w_s=D-(1-2S)L in Fig. 1(b)), then, as in the static case, the capacitance decreases [13]. Even the capacitance due to the Floquet modes becomes smaller, as the area of the parallel plate capacitor formed by fractal patch and ground plane gradually decreases by a factor ($1-4S^2$). Conversely, by increasing the patch length L from 62mm up to 79mm, for a fixed S-value, the cell resonant frequency decreases, as expected. Furthermore, the overall cell capacitance grows up (Table I), due to the growing metalized area inside the cell (Floquet modes capacitance) and the decreasing distance between adjacent elements (i.e. w=D-L in Fig. 1(b)). For this reason, the unit cell impedance gradually increases, so compromising the free-space matching condition. In conclusion, a proper tuning of both fractal sizes, L and S, leads to the perfect matching between MA cell and free space, offering a certain degree of miniaturization with respect to the square shape. The foregoing considerations provide design guidelines for the proposed fractal MA. The above analysis results, in fact, are properly exploited to define

a graphical synthesis procedure for designing a UHF-fractal MA cell (Fig. 3). The procedure allows to find the best L and S values able to simultaneously meet the following goals: f_0=868MHz, $\mathrm{Re}\{Z_{cell}^{res}\} = 377\Omega$. Both the substrate as well as the cell size D are fixed. A family of curves is derived from analysis data (Fig. 3(a)), representing the real part of the resonant input impedance of the cell versus the corresponding resonant frequency, for different patch size L and by varying the scaling factor S. The corresponding curves family relating the cells resonant frequency and the scaling factor S, computed for each considered L-value, is reported in Fig. 3(b). At first, a target point TP is obtained on Fig. 3(a) as the intersection of two straight lines representing the above defined synthesis goals. Then, the curve passing through the point TP is selected among those depicted in Fig. 3(a), so achieving the optimal patch length L_{opt}. Finally, by projecting TP onto the curve labeled with L_{opt} and belonging to the family depicted in Fig. 3(b), the optimal scaling factor S_{opt} is computed. Fig. 3 shows that the best absorption is achieved at 868 MHz, when L_{opt} and S_{opt} are respectively equal to 67mm and 0.21. In this last case, a very good matching is realized between Z_{cell} and free space (Fig. 2(a)), giving an absorptivity peak greater than 99.9% (Fig. 2(b)). As a further analysis, a good angular stability is demonstrated for both TE and TM polarizations. To this end, the absorption coefficients versus frequency are computed for different incidence angles θ_i, showing very high peak values, ranging from 87% up to 99.8% (Fig. 4).

TABLE I
GEOMETRICAL AND ELECTRICAL PROPERTIES OF ABSORBER UNIT CELLS.

	L= 62mm				L= 67mm				L= 79mm			
S	0	0.15	0.25	0.3	0	0.15	0.21	0.3	0	0.15	0.25	0.3
R_p (Ω)	1.16	1.4	1.87	2.29	0.93	1.11	1.32	1.8	0.58	0.69	0.94	1.15
L_p (nH)	4.49	7.2	14.3	21.5	3.4	5.75	9	17.3	1.69	3.5	7.74	12.35
C_p (pF)	2.35	2.14	1.84	1.7	3.15	2.88	2.59	2.32	5.86	5.23	4.6	4.28
$\mathrm{Re}\{Z_{cell}^{res}\}(\Omega)$	711	488	250	161	755	525	375	183	840	600	317	199
f_{res}(MHz)	1124	1030	868	761	1042	950	868	717	868	800	684	600

IV. MINIATURIZATION OF THE ABSORBER UNIT CELL

As demonstrated in the previous section, the proposed Minkowski geometry allows to reduce the patch size, leaving unchanged the substrate features, so offering very small inter-element spacing D [11, 12]. The above feature avoids grating lobes occurrences in reflectarrays [11, 15, 16], and allows to reduce the sizes of MAs for those applications operating in restricted indoor environments. The intrinsic miniaturization capabilities of fractal shapes are exploited in this Section to design miniaturized MA cells for the UHF-RFID band. By following the design rules outlined in Section III and adopting the design curves reported in Fig. 5(a), a set of 868MHz fractal MA cells is designed, with progressively reduced sizes D, ranging from $0.3\lambda_0$ down to $0.15\lambda_0$. The absorptivity and the sizes of each designed cell are depicted in Fig. 5(b). It can be easily observed that a proper tuning of both patch geometric parameters, L and S, assures a perfect absorption at the same desired frequency ($A(\omega_0)$>99%), for all considered cases.

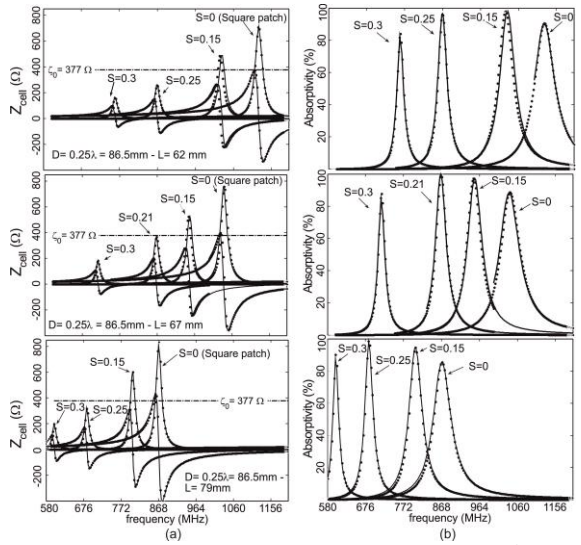

Fig. 2. Full-wave simulations (—) and TL model results (· · ·) of Minkowski unit cells having D= λ/4 and L equal to 62mm, 67mm and 79mm: (a) Input impedance and (b) Absorptivity vs. frequency for different scaling factor S.

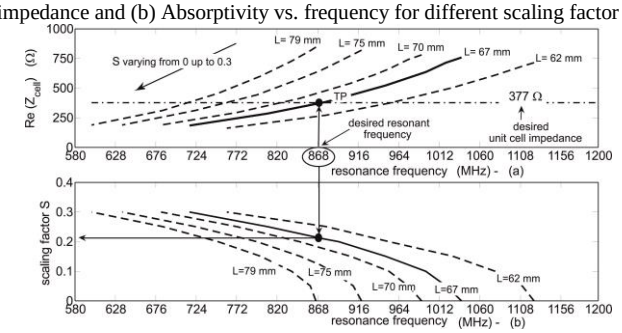

Fig. 3. Synthesis of a Minkowski MA unit cell (D= λ/4, h=3.2mm, ε_r=4.4, tanδ=0.02): (a) cell input impedance *vs* resonant frequency for different patch size L and variable scaling factor S; (b) scaling factor *vs* unit cell resonant frequency for different patch size L.

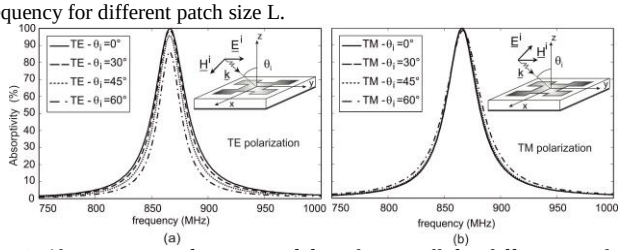

Fig. 4. Absorptivity *vs* frequency of fractal unit cell for different incidence angles (L=67mm, S=0.21): (a) TE-polarization, (b) TM-polarization.

In fact, as discussed in the previous section, the inherent higher capacitive coupling due to smaller unit cell sizes can be properly reduced through the use of a fractal patch having a smaller length L and a greater scaling factor S (Fig. 5(a)), keeping unit cells capacitance constant and equal to a value of about 2.65÷2.7 pF (Fig. 5(d)). In this way, the resonant input impedance remains well matched to the free space at 868MHz, for each considered cell size D (Fig. 5(d)), thus confirming the effectiveness of the proposed configuration in designing smaller UHF MA panels. In order to better appreciate the miniaturization capabilities of the proposed configuration, the above results are compared with the behavior of a standard square patch [5], printed on the same substrate. Fig. 5(a) clearly shows that the use of square patches (i.e. S=0) having the same sizes (i.e. L×L) of the corresponding 868MHz-fractal cells gives greater resonance frequencies, as the effective

electrical length of the square elements is smaller with respect to that of fractal ones [12]. As a matter of fact, Fig. 5(c) shows how the absorption peaks of the square patches shift up to 952MHz, for D=0.3λ-L=73.5mm, and to 1040MHz, for D=0.25λ-L=67mm. In order to move the resonance/absorption condition down to the desired working frequency, the square-based cells must be resized using greater L-values (i.e. D=0.3λ-L=80.6mm, D=0.25λ-L=79mm Fig. 5(a, c)). However, the combined use of smaller grid spacings and greater patch sizes enhances the value of the resonant input impedance Fig. 5(d), thus leading to a non-optimal absorption Fig. 5(c). In fact, whilst for the case D=0.4λ_0 the square-based cell impedance is nearly equal to the free space ones (i.e. $\mathrm{Re}\{Z_{cell}^{res}\} \cong 360\Omega$), so giving perfect absorption (Fig. 5(c)), in the case of smaller cell sizes the higher capacitive coupling between adjacent patches and between the patches and the ground plane gives rise to very high resonant input impedances (i.e. $\mathrm{Re}\{Z_{cell}^{res}\}$ =615Ω for D=0.3λ_0 and 840Ω for D=0.25λ_0), that are mismatched with the free space (Fig. 5(d)). Thus, the absorptivity of the designed square based cells results to be lower than 85%, for D smaller than 0.25λ_0 (Fig. 5(c)). Finally the use of smaller cells (D<0.25λ_0), makes the design of 868MHz-square patches unfeasible, as the required resonant length values are greater with respect to the cell sizes D (Fig. 5(a)). In conclusion, the proposed configuration allows to work with a unit cell size D that is 50% smaller with respect to a standard square-based configuration, ensuring very high absorption performances. Similar conclusions can be drawn when the proposed fractal MA is compared with a low capacitive cross shape. As a matter of the fact, the resonance of a cross element printed on the same substrate, having the same length L of the designed fractal patches, moves up to 1055MHz, when D=0.3λ-L=73.5mm, and to 1170MHz, when D=0.25λ-L=67mm (a cross thickness equal to 1/8 of cell periodicity D is fixed [13]), thus showing lower miniaturization skills with respect to the proposed fractal shape.

V. Conclusions

A Minkowski fractal shape has been proposed in this work to design a thin and compact MA panel for multipath mitigation in UHF-RFID systems. The adopted configuration has been extensively analyzed through the combined use of a commercial full-wave code and an equivalent circuit model. Useful design rules have been retrieved from an extensive analysis stage. Furthermore, quite good angular stability, high miniaturization capabilities (about 50% with respect to standard configurations) and very large absorption percentages have been demonstrated, making the proposed configuration appealing for those applications operating in restricted indoor areas, such as RFID systems. As future developments, the miniaturization capabilities of the proposed configuration will be exploited to design multiband MAs.

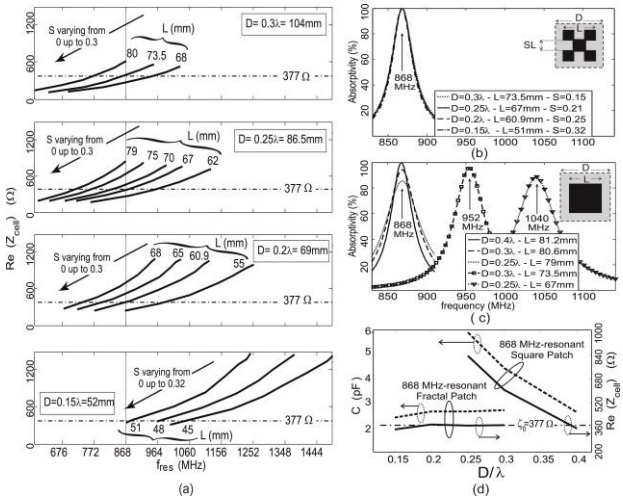

Fig. 5. MA cell having a decreasing size D: (a) input impedance *vs* resonant frequency for different patch size L, by varying the scaling factor S; (b) absorptivity vs frequency – fractal cell; (c) absorptivity vs frequency – square-based cell; (d) unit cell capacitance and resonant input impedance *vs* D/λ.

References

[1] A.A. Saleh, R.A. Valenzuela, "A statistical model for indoor multipath propagation", IEEE J. Sel. Areas Comm.,vol. 5,no. 2, pp. 128-137, 1987.

[2] A. Lazaro, D. Girbau, D. Salias, "Radio link budgets for UHF RFID on multipath environments", IEEE Trans. Antennas Propag., vol. 57, no. 4, pp. 1241-1251, 2009.

[3] S. Costanzo, A. Costanzo, A. Raffo, A. Borgia, "Environmental effects on the performances of a UHF passive tag-based commercial RFID system", WorldCIST 2016, Advances in intelligent systems and computing, vol. 445, Springer, doi: 10.1007/978-3-319-31307-8_35.

[4] Y. Okano, S. Ogino, K. Ishikawa, "Development of optically transparent ultrathin microwave absorber for ultrahigh-frequency RF identification system", IEEE Trans. Microw. Theory Tech., vol. 60, no. 8, 2012.

[5] F. Costa, S. Genovesi, A. Monorchio, G. Manara, "Low-cost metamaterial absorbers for sub-GHz wireless systems", IEEE Antennas and Wireless Prop. Letters, 13, pp. 27-30, 2014.

[6] F.Costa, S. Genovesi, A. Monorchio, G. Manara, "Perfect metamaterial absorbers in the ultra-high frequency range", Internat. Symp. on Electromagnetic Theory, Hiroshima, 2013.

[7] W. Zuo, Y. Yang, X. He, D. Zhan, Q. Zhang, "A miniaturized metamaterial absorber for ultrahigh-frequency RFID system", IEEE Antennas and Wireless Propag. Letters, 16, pp. 329-332, 2017.

[8] N.I. Landy, S. Sajuyigbe, J.J. Mock, D.R. Smith, W.J. Padilla, "Perfect metamaterial absorber", Phys. Rev. Lett., vol. 100, no. 20, 2008.

[9] C.M. Watts, X. Liu, W.J. Padilla, "Metamaterial electromagnetic wave absorbers", Adv. Mater., 24, pp. 98-120, 2012.

[10] F. Venneri, S. Costanzo, "Fractal microwave absorbers for multipath reduction in UHF-RFID systems", WorldCIST 2017, Advances in Intelligent Systems and Computing, vol. 570, Springer, Cham, doi: 10.1007/978-3-319-56538-5_100.

[11] S. Costanzo, F. Venneri, "Miniaturized fractal reflectarray element using fixed-size patch", IEEE Antennas and Wireless Propag. Letters, 13, pp. 1437-1440, 2014.

[12] S. Costanzo, F. Venneri, G. Di Massa, A. Borgia, A. Costanzo, A. Raffo, "Fractal reflectarray antennas: state of art and new opportunities", International Journal of Antennas and Propagation, Article ID 7165143, 2016, doi:10.1155/2016/7165143.

[13] F. Costa, S. Genovesi, A. Monorchio, G. Manara, "A circuit-based model for the interpretation of perfect metamaterial absorbers", IEEE Trans. on Antennas and Propag., vol. 61, no. 3, pp. 1201-1209, 2013.

[14] O. Luukkonen, C. Simovski, G. Granet, G. Goussetis, D. Lioubtchenko, A. V. Räisänen, and S. A. Tretyakov, "Simple and accurate analytical model of planar grids and high-impedance surfaces comprising metal strips or patches", IEEE Trans. Antennas Propag.,vol. 56, no. 6, 2008.

[15] F. Venneri, S. Costanzo, G. Di Massa, "Tunable reflectarray cell for wide angle beam-steering radar applications", Journal of Electrical and Computer Engineering, vol. 2013, Article ID 325746, 7 pages, 2013. doi:10.1155/2013/325746.

[16] S. Costanzo, F. Venneri, A. Raffo, G. Di Massa, P. Corsonello, "Radial-shaped single varactor-tuned phasing line for active reflectarrays", IEEE Transactions on Antennas and Propagation, vol. 64, no. 7, pp. 3254-3259, July 2016. doi: 10.1109/TAP.2016.2562673.